哈爾濱工業大學
HARBIN INSTITUTE OF TECHNOLOGY

DEM Numerical simulation of two-component particles flow characteristics in a magnetically controlled bubbling bed

Reporter：Biao Wang

Academic advisor：Prof. Yurong He

2019.5.29 Guilin, China

CATALOGUE

CATALOGUE

Background

Magnetically fluidized bed

- The magnetic field was added to the ordinary fluidized bed as the external energy field, and the solid particles were magnetic particles

Application

- **In the chemical**: Ferromagnetic materials catalyze, the biochemical reaction of ferromagnetic particles as carriers
- **In the physical**: Filter, Dust removal, Sorting the material, Fluidized viscous particles, Particle transport under microgravity

Advantages

- Small vibration
- Little noise
- Solid particle handling is convenient
- High mass and heat transfer rate

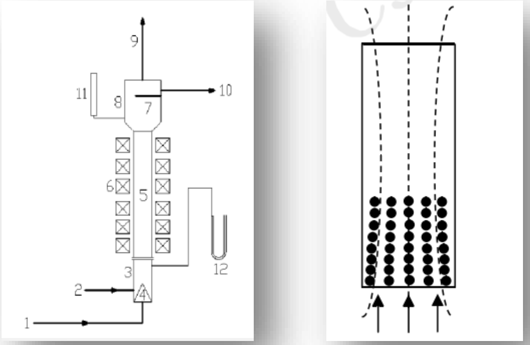

magnetic field fluidized bed

Background

- The lipase was immobilized on magnetized chitosan microspheres to produce biodiesel（Zhou, etc. 2014）
- The reaction enzyme is fixed on the magnetic particle for catalysis（Bahar, etc. 2000）
- Application of the magnetically fluidized bed in coal washing（Mohanta, etc. 2013）
- Waste treatment in magnetically fluidized bed under microgravity（Sornchamni, etc. 2005）

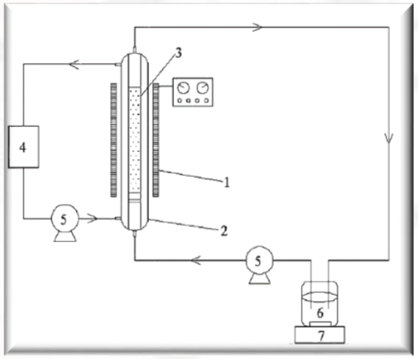

Magnetically stable fluidized bed reactor

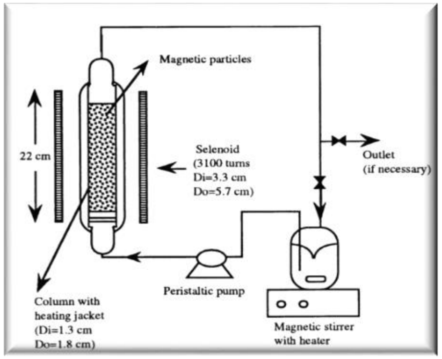

Magnetically stable fluidized bed biodiesel reactor

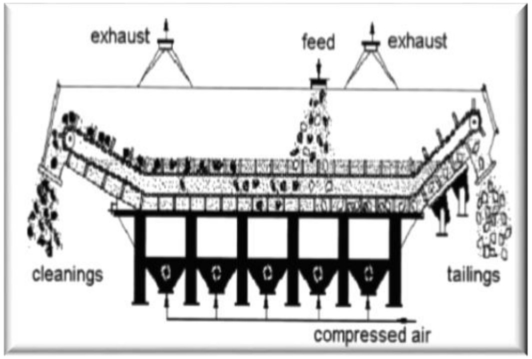

Schematic diagram of pulverized coal separator

Zhou G X. Biotechnology Letters, 2014, 36(1): 63-68.
Mohanta S. Particulate Science and Technology, 2013, 31(1): 16-27.
Bahar T. Enzyme and Microbial Technology,2000,26(1): 28-33.
Sornchamni T. Industrial & Engineering Chemistry Research, 2005, 44(24): 9199-9207.

Background

Brief summary

- At present, the magnetically fluidized bed has been used in environment, energy, aviation, chemical catalysis and other fields. It has high development value and broad application prospect
- There are still some limitations in the study of magnetically fluidized bed. The research mainly focuses on single-component solid particles, and there are few numerical simulation studies on the fluidization of two-component particles in magnetic field

Research contents

- Based on DEM model, the mathematic model under the action of magnetic field force is established
- Flow characteristics of single component particles under uniform and gradient magnetic fields were analyzed
- Separation characteristics of two - component particles in gradient magnetic field

CATALOGUE

Mathematic model

Gas phase

Mass-conservation equation

$$\frac{\partial}{\partial t}\left(\varepsilon_{g}\rho_{g}\right)+\nabla\cdot\left(\varepsilon_{g}\rho_{g}\boldsymbol{u}_{g}\right)=0$$

Moment-conservation equation

$$\frac{\partial}{\partial t}\left(\varepsilon_{g}\rho_{g}\boldsymbol{u}_{g}\right)+\nabla\cdot\left(\varepsilon_{g}\rho_{g}\boldsymbol{u}_{g}\boldsymbol{u}_{g}\right)=-\varepsilon_{g}\nabla p-\nabla\cdot\left(\varepsilon_{g}\boldsymbol{\tau}_{g}\right)-\boldsymbol{F}_{gp}+\varepsilon_{g}\rho_{g}\mathbf{g}$$

Viscous stress tensor

$$\boldsymbol{\tau}_{g}=\frac{2}{3}\mu_{g}\left(\nabla\cdot\boldsymbol{u}_{g}\right)\mathbf{I}-\mu_{g}\left[\left(\nabla\boldsymbol{u}_{g}\right)+\left(\nabla\boldsymbol{u}_{g}\right)^{T}\right]$$

Unit tensor

$$\mathbf{I}=\begin{bmatrix}1&0&0\\0&1&0\\0&0&1\end{bmatrix}$$

ρ_g-gas phase density（kg/m^3）　$\boldsymbol{F}_{gp}$-interphase momentum exchange rate（kg/(m^2 s^2)）

μ_g-gas phase shear viscosity（Pa s）　ε_g-gas phase fraction（-）　$\boldsymbol{u}_g$-gas phase shear viscosity（m/s）

$\mathbf{g}$-gravitational acceleration　（m^2/s）

Mathematic model

Solid phase

The motion of individual particles is obtained by solving Newton’s second law of motion

Dynamic equations for the translational motion of particles

$$m_p \frac{d^2 \boldsymbol{r}}{dt^2} = -V_p \nabla p + \frac{V_p \beta}{1-\varepsilon_g}\left(\boldsymbol{u}_g - \boldsymbol{v}_p\right) + m_p \boldsymbol{g} + \boldsymbol{F}_c + \boldsymbol{F}_m$$

m_p-particle mass（kg） $\boldsymbol{v}_p$-particle velocity（m/s） t-time（s）

V_p-particle volume（m^3） β-drag coefficient（kg/(m^3 s)）

ε_g-gas phase fraction（-） $\boldsymbol{F}_c$-contact force（N）

$\boldsymbol{F}_m$-magnetic force（N）

Dynamic equations for the rotations of particles

$$I_p \frac{d\boldsymbol{\omega}_p}{dt} = \boldsymbol{T}_p$$

I_p-moment of inertia（kg m²） $\boldsymbol{T}_p$-torque（N m）

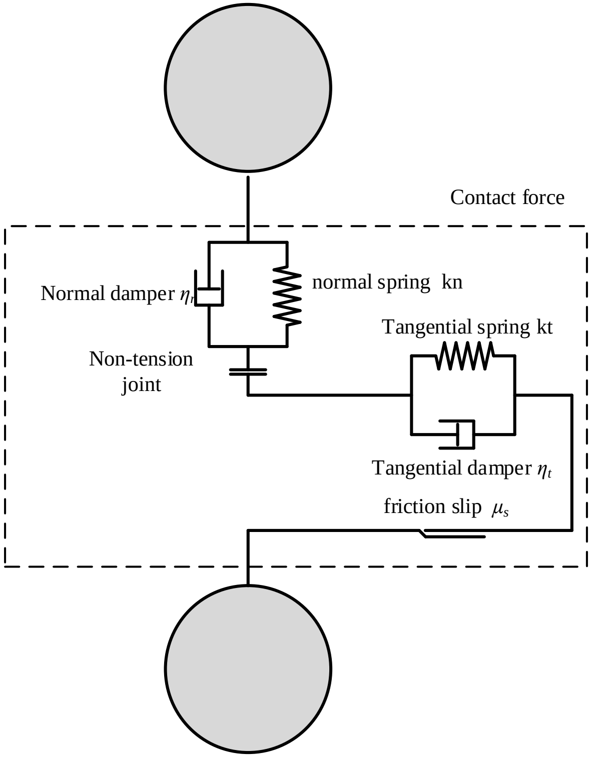

spring-damping model

Mathematic model

Contact force

- The spring component obeying Hooke's law is used to describe the elastic deformation of the particle.（Conservation of energy）
- The dampers associated with particle velocity are used to consider attenuation effects.（Energy dissipation）

Normal component

$$\boldsymbol{F}_{\mathbf{n}} = -k_{\mathbf{n}}\boldsymbol{\delta}_{\mathbf{n}} - \eta_{\mathbf{n}}\boldsymbol{v}_{\mathbf{n}}$$

Tangential component

$$\boldsymbol{F}_{\mathbf{t}} = \begin{cases} -k_{\mathbf{t}}\boldsymbol{\delta}_{\mathbf{t}} - \eta_{\mathbf{t}}\boldsymbol{v}_{\mathbf{t}} & \left|\boldsymbol{F}_{\mathbf{t}}\right| \le \mu_f \left|\boldsymbol{F}_{\mathbf{n}}\right| \\ -\mu_f \left|\boldsymbol{F}_{\mathbf{n}}\right| \dfrac{\boldsymbol{v}_{\mathbf{t}}}{\left|\boldsymbol{v}_{\mathbf{t}}\right|} & \left|\boldsymbol{F}_{\mathbf{t}}\right| > \mu_f \left|\boldsymbol{F}_{\mathbf{n}}\right| \end{cases}$$

k- spring coefficient（N/m） η- damping coefficient（N s/m） $\boldsymbol{\delta}$- overlap（m） **t**-tangential（-）

$\boldsymbol{v}_{\mathrm{t}}$-tangential relative velocity（m/s） μ_{f}-friction coefficient（-） **n**-normal（-）

Mathematic model

Magnetic force

The component resulting from external magnetic field gradients

$$\boldsymbol{F}_{\mathrm{me}} = \mathrm{V}_{\mathrm{P}}\mu_0\chi_e H\nabla H$$

The component resulting from magnetized particles

$$\boldsymbol{F}_{\mathrm{mi}} = \boldsymbol{F}_r + \boldsymbol{F}_\theta$$

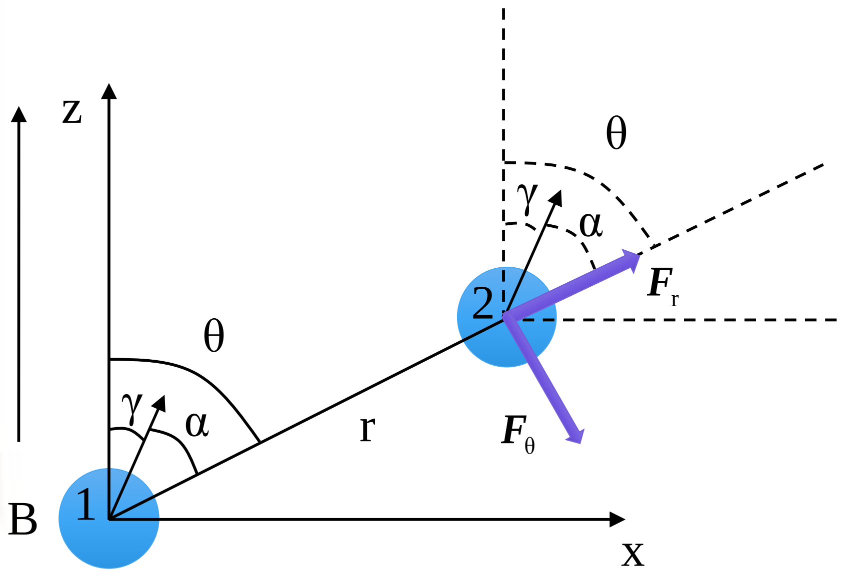

The interactions between magnetized particles

Mathematic model

Magnetic force

$$\boldsymbol{F}_{\mathrm{r}} = -\frac{\mu_0}{4\pi}\left\{\frac{m^2}{r^3}\left[-6\cos(\theta-\gamma)\sin(\theta-\gamma)\right]\frac{\partial\gamma}{\partial r}+\left[1-3\cos^2(\theta-\gamma)\right]\left(-\frac{3m^2}{r^4}+\frac{2m}{r^3}\frac{\partial m}{\partial r}\right)\right\}$$

$$\frac{\partial\gamma}{\partial r} = -\frac{9a\sin 2\theta}{r\left\{\left[1+a(3\cos 2\theta-1)\right]^2+(3a\sin 2\theta)^2\right\}}$$

$$\frac{\partial m}{\partial r} = \frac{\chi_e V_p B\left\{\left[(1-a)\sin\gamma+3a\sin(2\theta-\gamma)\right]\frac{\partial\gamma}{\partial r}-\frac{3a}{r}\left[\cos\gamma+3\cos(2\theta-\gamma)\right]\right\}}{\mu_0\left\{\cos\gamma-a\left[\cos\gamma+3\cos(2\theta-\gamma)\right]\right\}^2}$$

$$\boldsymbol{F}_{\theta} = -\frac{\mu_0}{4\pi r^4}\left\{6m^2\cos(\theta-\gamma)\sin(\theta-\gamma)\left(1-\frac{\partial\gamma}{\partial\theta}\right)+2m\left[1-3\cos^2(\theta-\gamma)\right]\frac{\partial m}{\partial\theta}\right\}$$

$$\frac{\partial\gamma}{\partial r} = \frac{2(3a\sin 2\theta)^2+6a\cos 2\theta\left[1+a(3\cos 2\theta-1)\right]}{\left[1+a(3\cos 2\theta-1)\right]^2+(3a\sin 2\theta)^2}$$

$$\frac{\partial m}{\partial\theta} = \frac{\chi_e V_p B\left\{\left[(1-a)\sin\gamma+3a\sin(2\theta-\gamma)\right]\frac{\partial\gamma}{\partial\theta}-6a\sin(2\theta-\gamma)\right\}}{\mu_0\left\{\cos\gamma-a\left[\cos\gamma+3\cos(2\theta-\gamma)\right]\right\}^2}$$

V_p-particle volume（m^3） μ_0-magnetic permeability of free space（N/A^2）

χ_e-particle effective magnetic susceptibility，$\chi_e = \frac{3\chi_p}{3+\chi_p}$ H -magnetic field intensity（A/m）

Mathematic model

Drag force

The interphase momentum exchange rate

$$\boldsymbol{F}_{\mathrm{gp}} = \frac{1}{V_{\mathrm{cell}}} \sum_{n=1}^{N_{\mathrm{p}}} \frac{\mathrm{V}_{\mathrm{p}}^{n} \beta}{1-\varepsilon_{\mathrm{g}}} \left(\boldsymbol{u}_{\mathrm{g}} - \boldsymbol{v}_{\mathrm{p}}^{n}\right)$$

The drag coefficient

$\varepsilon_g \leqslant 0.8$

$$\beta_{\mathrm{Ergun}} = 150 \frac{\left(1-\varepsilon_{\mathrm{g}}\right)^{2} \mu_{g}}{\varepsilon_{\mathrm{g}} \mathrm{d}_{\mathrm{p}}^{2}} + 1.75 \frac{\left(1-\varepsilon_{\mathrm{g}}\right) \rho_{\mathrm{g}} \left|\boldsymbol{u}_{\mathrm{g}} - \boldsymbol{v}_{\mathrm{p}}^{\mathrm{n}}\right|}{\mathrm{d}_{\mathrm{p}}}$$

$\varepsilon_g > 0.8$

$$\beta_{\mathrm{Wen\&Yu}} = \frac{3}{4} \rho_{\mathrm{g}} C_{D} \frac{\left(1-\varepsilon_{\mathrm{g}}\right) \varepsilon_{\mathrm{g}}^{-1.7}}{\mathrm{d}_{\mathrm{p}}} \left|\boldsymbol{u}_{\mathrm{g}} - \boldsymbol{v}_{\mathrm{p}}^{\mathrm{n}}\right|$$

Drag coefficient

$$C_{D} = \begin{cases} \dfrac{24}{Re}\left(1+0.15 Re^{0.687}\right) & Re < 1000 \\ 0.44 & \mathrm{Re} \geq 1000 \end{cases}$$

Reynolds number

$$Re = \frac{\rho_{\mathrm{g}} \varepsilon_{\mathrm{g}} d_{\mathrm{p}} \left|\boldsymbol{u}_{\mathrm{g}} - \boldsymbol{v}_{\mathrm{p}}\right|}{\mu_{\mathrm{g}}}$$

CATALOGUE

Model validation

Initial conditions and boundary conditions

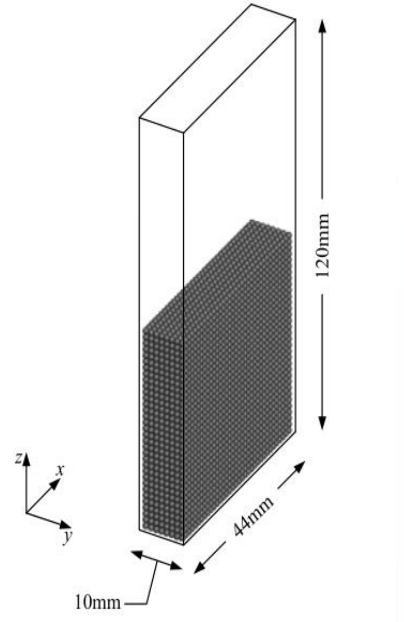

- Pressure outlet boundary condition is adopted at the top
- No slip boundary condition is adopted at the wall surface
- Particles have the same diameter and density
- The simulation lasted for 15s

Simulation parameters

Variables	Value	unit
Fluidized bed（3D）		
Geometry size ($L_x \times L_y \times L_z$)	44×120×10	mm
Meshes ($N_x \times N_y \times N_z$)	12×24×3	-
Particles		
Particle number N_p	9240	-
Particle diameter d_p	1.2	mm
Particle density	1000	kg/m^3
Recovery coefficient e	0.97	-
Sliding friction coefficient μ_f	0.1	-
Normal spring stiffness $\mu_{f'}$	0.3	-
Normal spring stiffness k_n	800	N/m
Tangential spring stiffness k_t	229	N/m
Gas		
Temperature	298.15	K
Gas density ρ_g	1.166	kg/m^3
Gas viscosity μ	1.82×10^{-5}	Pa·s
Fluidization gas velocity U_{bg}	0.9	m/s
Outlet pressure	1.01325×10^{5}	Pa

Müller C R, Holland D J, Sederman A J, et al. *Powder Technology*, 2008, 184(2): 241-253.

Model validation

Results

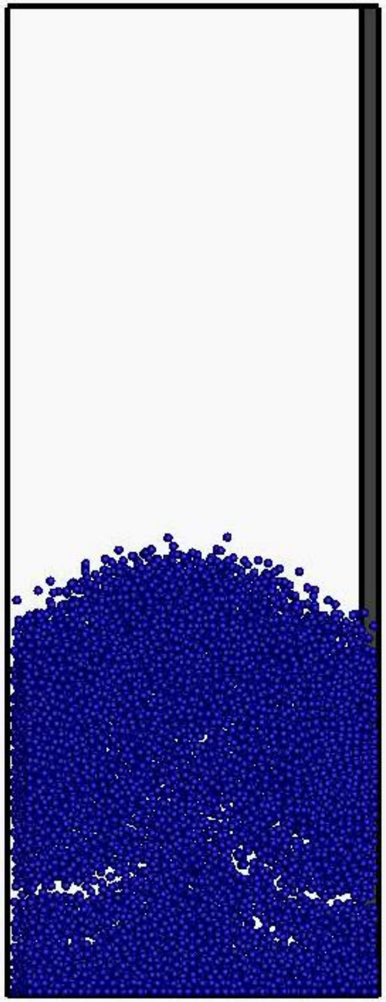

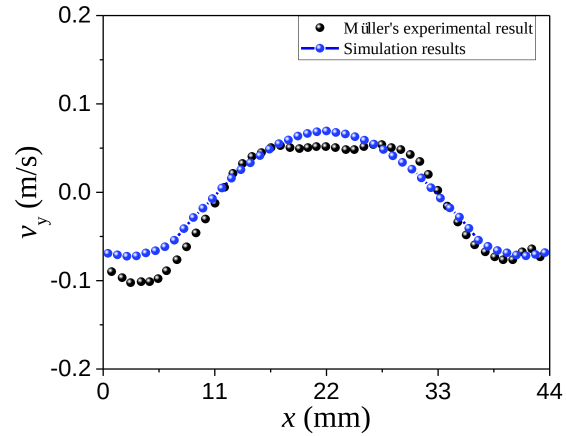

a） h = 10mm

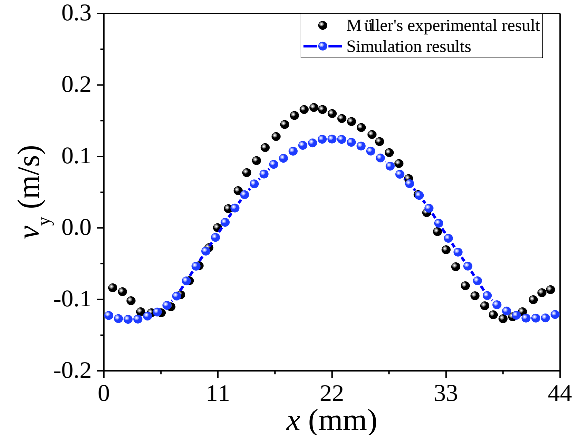

b） h = 20mm

- **Phenomenon：**
  - The numerical simulation results are in good agreement with the experimental data
  - At the bed of 20mm, the numerical simulation has underestimated the particle velocity in the central region
- **Analysis：**
  - The shape of particles affects the flow state of particles in fluidized bed, leading that the drag force is different

Single-component particle

☐ Initial conditions and boundary conditions

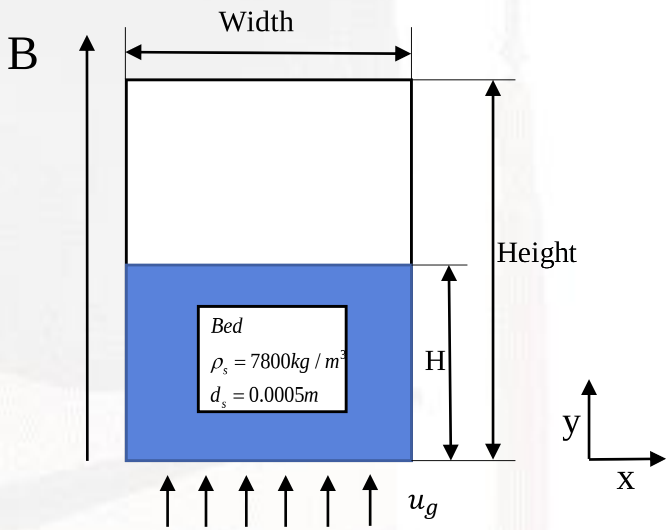

- Pressure outlet boundary condition is adopted at the top
- No slip boundary condition is adopted at the wall surface
- Particles have the same diameter and density
- The simulation lasted for 15s

Simulation parameters		
Variables	Value	unit
Fluidized bed（2D）		
Geometry size ($L_x \times L_y$)	22×52	mm
Meshes ($N_x \times N_y$)	11×20	-
Particles		
Particle number N_p	2002	-
Particle diameter d_p	0.5	mm
Particle density	7800	kg/m^3
Recovery coefficient e	0.9	-
Sliding friction coefficient μ_f	0.3	-
Normal spring stiffness $\mu_{f'}$	800	N/m
Normal spring stiffness k_n	229	N/m
Particle effective susceptibility χ_e	0.682	
Gas		
Temperature	298.15	K
Gas density ρ_g	1.166	kg/m^3
Gas viscosity μ	1.82×10^{-5}	Pa·s
Fluidization gas velocity U_{bg}	1.1	m/s
Outlet pressure	1.01325×10^5	Pa
Magnetic field	**Uniform magnetic field**	
Direction β	0/30/45/60/90	°
Magnetic induction intensity B	0.005/0.01/0.02	T

Single-component particle

Instantaneous particle spatial distribution

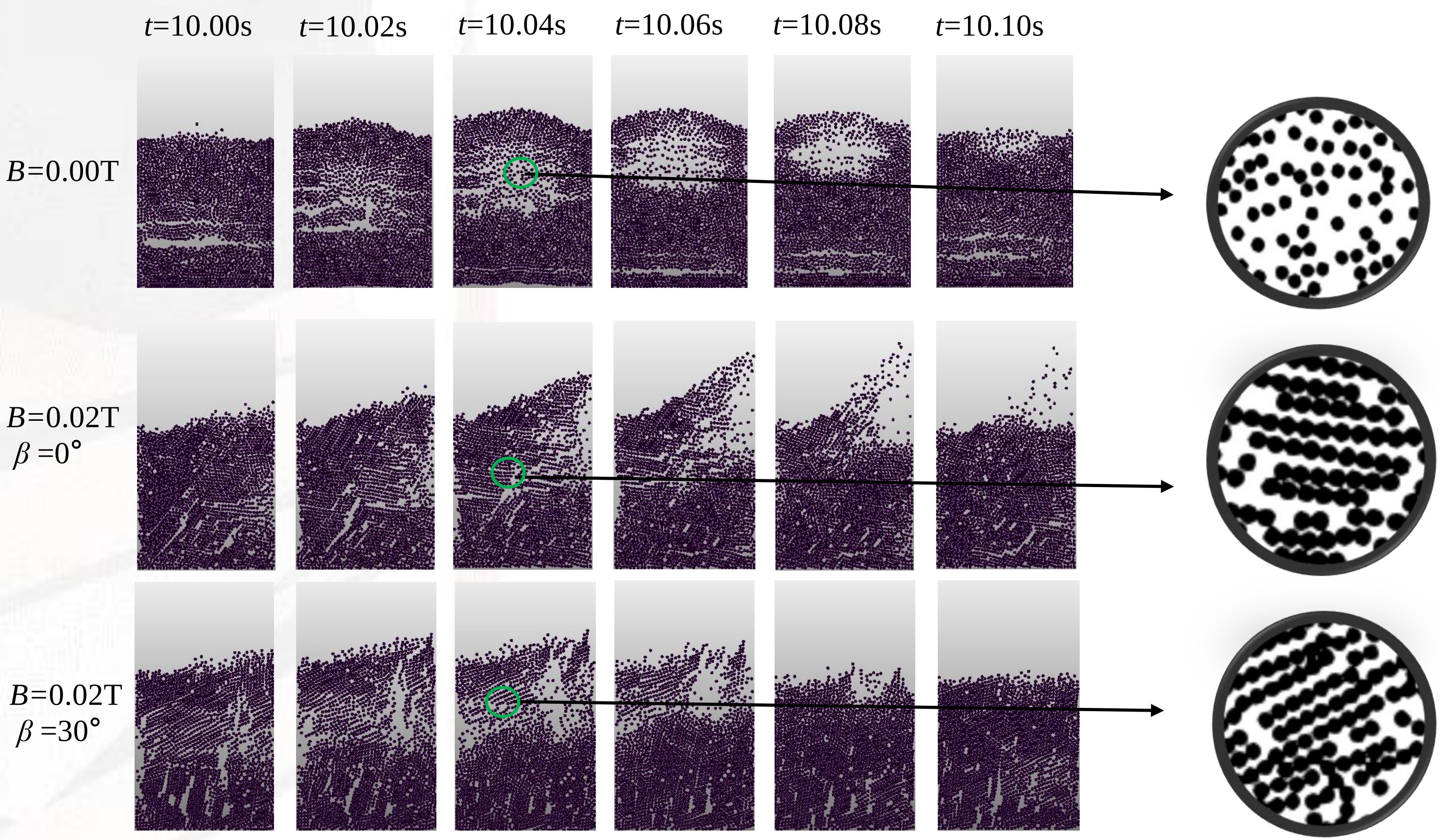

Single-component particle

☐ Instantaneous particle spatial distribution

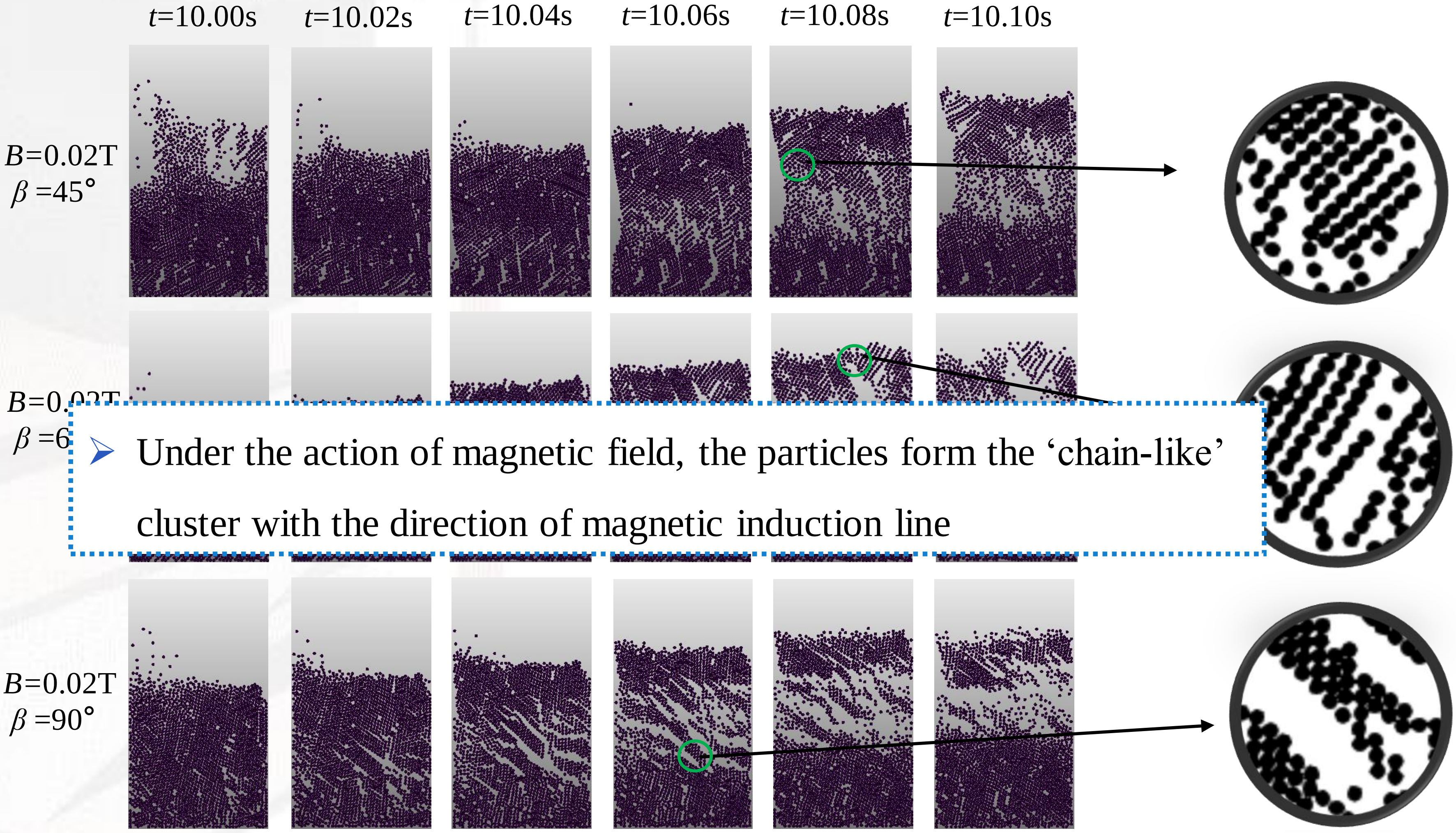

➢ Under the action of magnetic field, the particles form the ‘chain-like’ cluster with the direction of magnetic induction line

Single-component particle

◻ Instantaneous particle spatial distribution（30°）

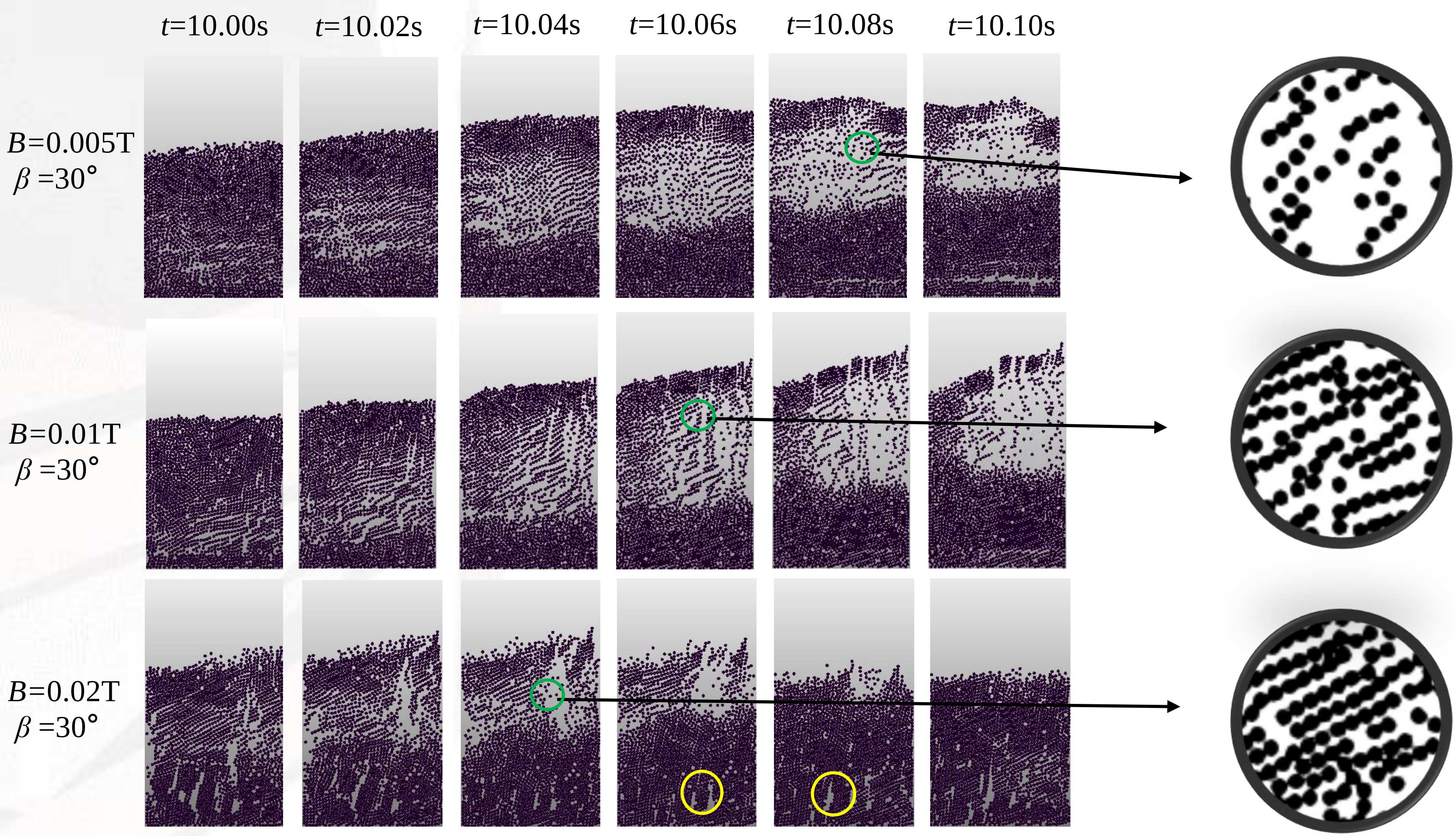

Single-component particle

Instantaneous particle spatial distribution（45°）

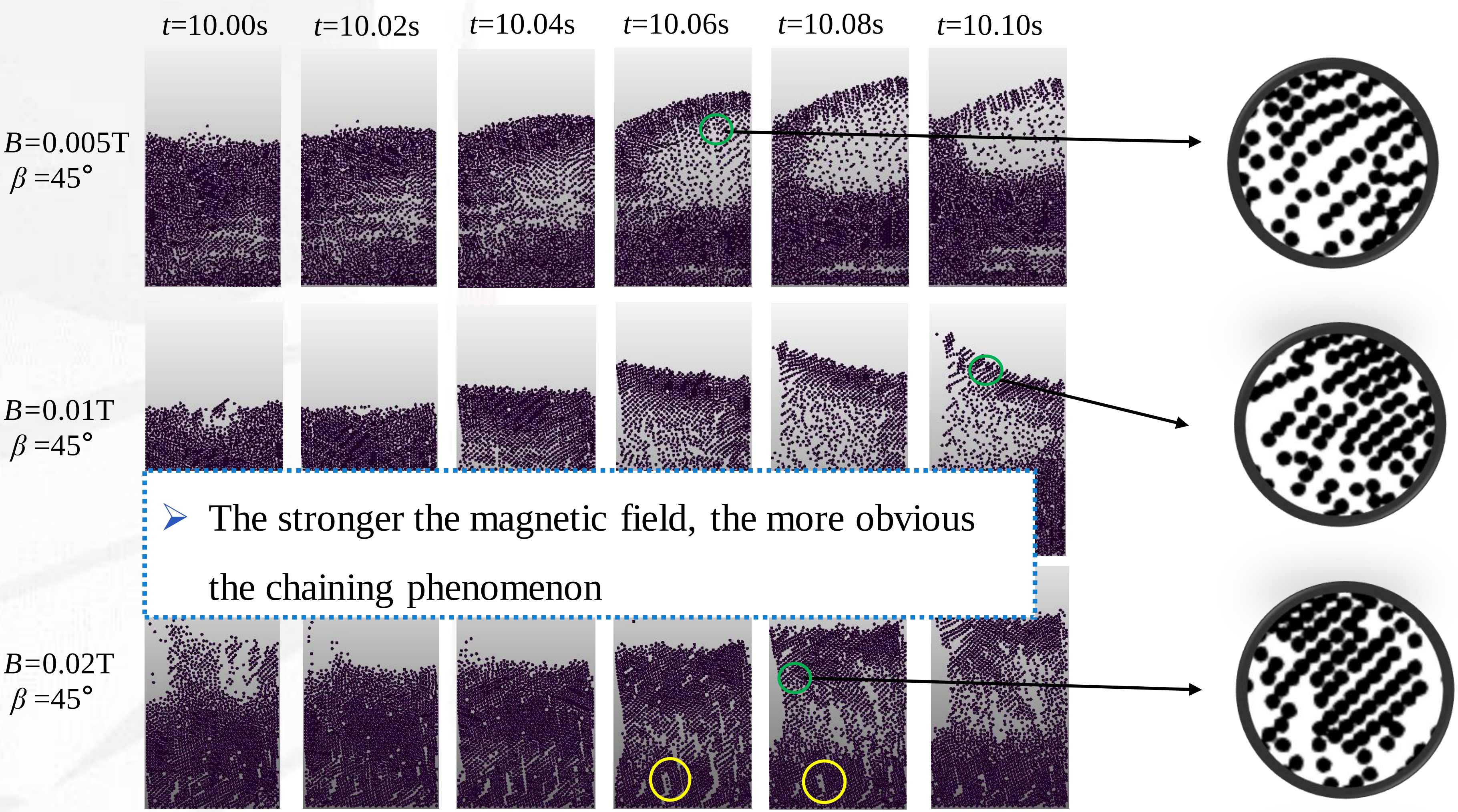

- The stronger the magnetic field, the more obvious the chaining phenomenon

Single-component particle

Gradient magnetic field

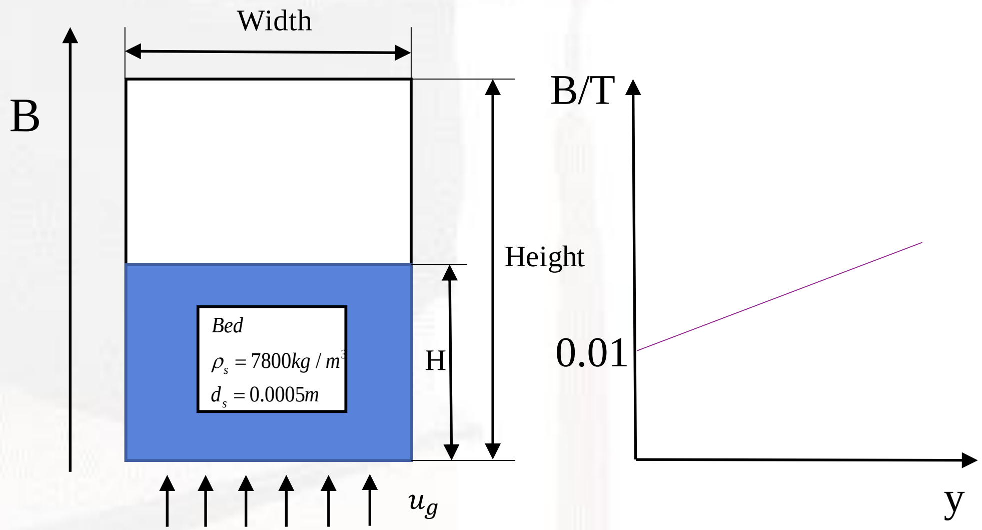

Pressure drop

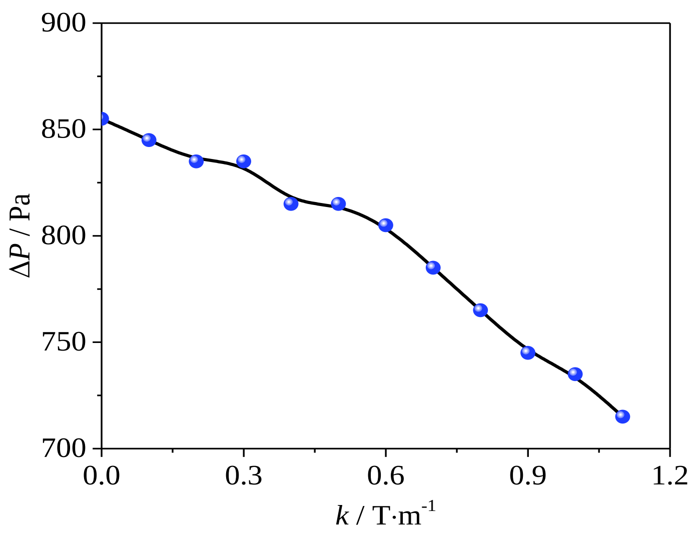

- **Phenomenon**
  - With the increase of magnetic field gradient, the pressure drop of bed decreases obviously
- **Analyze**
  - The external gradient magnetic force can offset part of the gravity of the particles. The direction of the force is the direction in which the magnetic field intensity increases.

Two-component particle

Initial conditions and boundary conditions

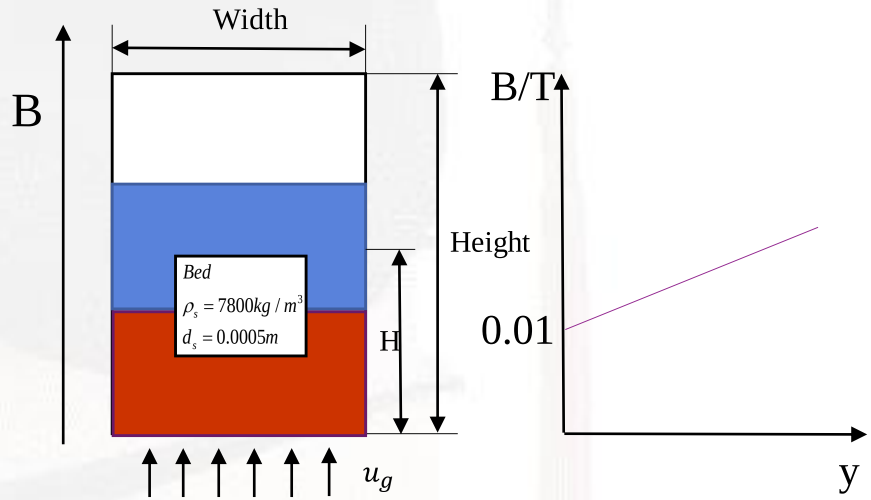

- Pressure outlet boundary condition is adopted at the top
- No slip boundary condition is adopted at the wall surface
- 2002 particles (1001 magnetic particles and 1001 non-magnetic particles).
- Particles have the same diameter and density
- The simulation lasted for 15s

Simulation parameters		
Variables	Value	unit
Fluidized bed（2D）		
Geometry size ($L_x \times L_y$)	22×52	mm
Meshes ($N_x \times N_y$)	11×20	-
Particles		
Particle number N_p	2002	-
Particle diameter d_p	0.5	mm
Particle density	7800	kg/m³
Recovery coefficient e	0.9	-
Sliding friction coefficient μ_f	0.3	-
Normal spring stiffness $\mu_{f'}$	800	N/m
Normal spring stiffness k_n	229	N/m
Particle effective susceptibility χ_e	0.682	
Gas		
Temperature	298.15	K
Gas density ρ_g	1.166	kg/m³
Gas viscosity μ	1.82×10^{-5}	Pa·s
Fluidization gas velocity U_{bg}	1.1	m/s
Outlet pressure	1.01325×10^5	Pa
Magnetic field	**Gradient magnetic field**	
Field intensity gradient k	0.8/0.9/1.0/1.1/1.2/1.3/1.4	T/m
Magnetic induction intensity at the air distribution plate B	0.01	T

Two-component particle

□ Instantaneous particle distribution - no magnetic

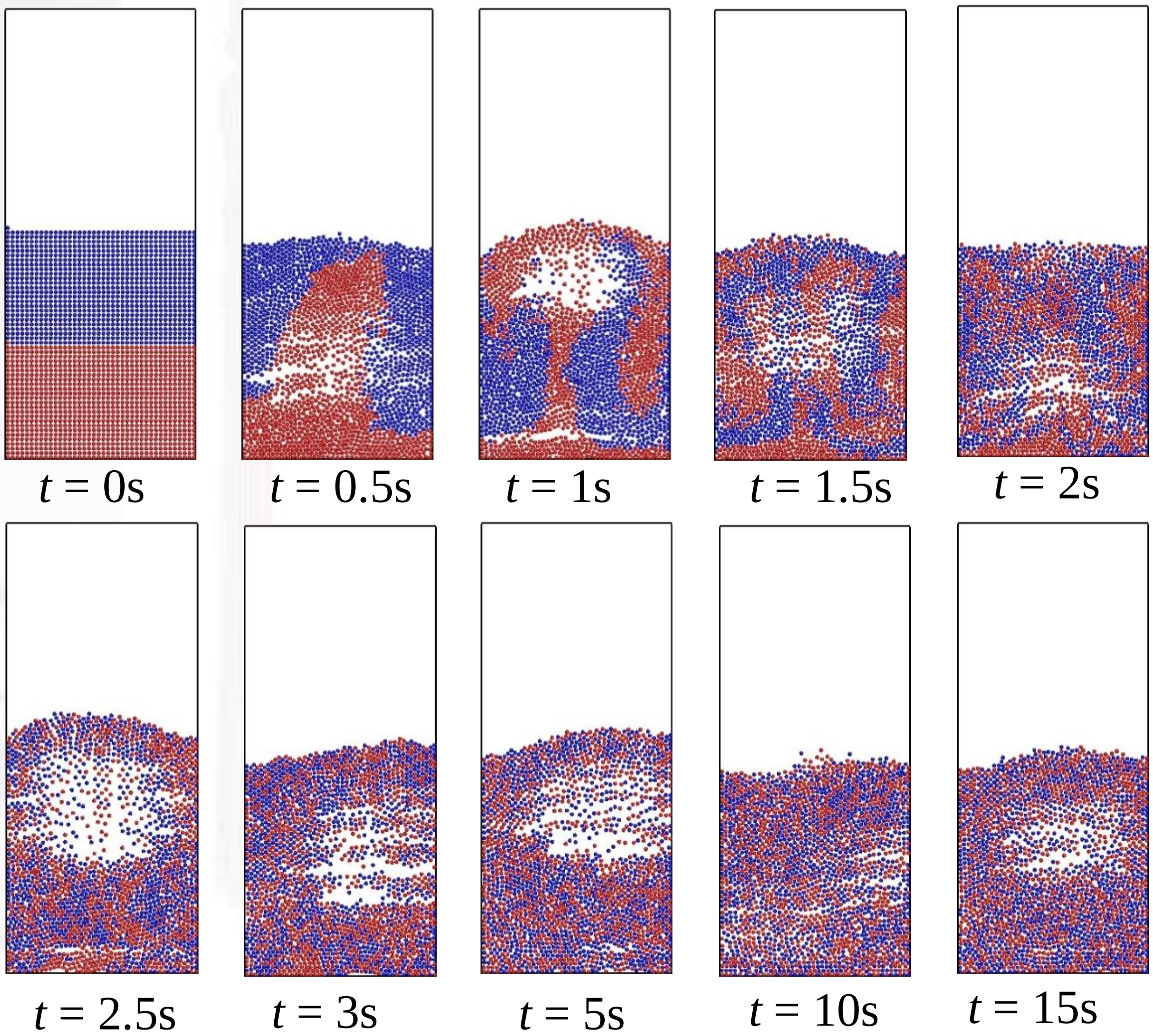

Two-component particle

Mixing index – no magnetic

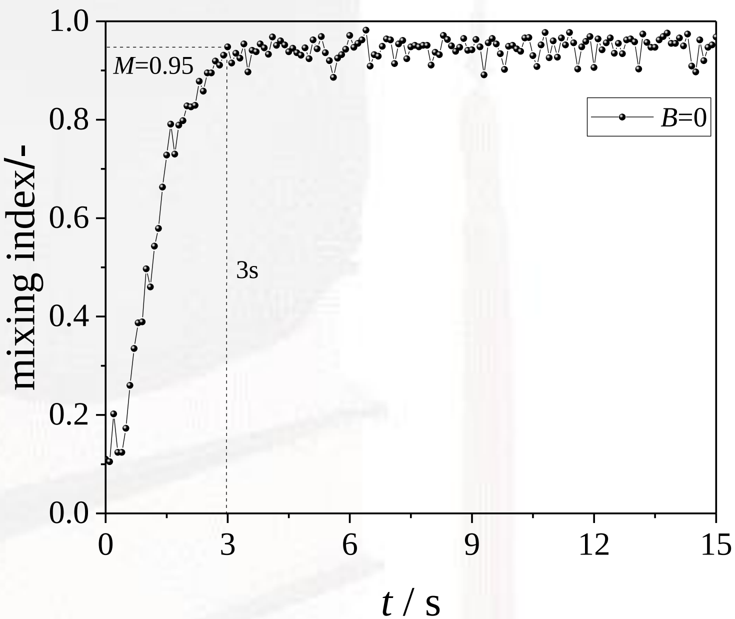

The change of particle mixing index with time

The variance based on sample particle composition

$$\sigma^2 = \frac{1}{N-1}\sum_{i=1}^{N}(c_i - \bar{c})$$

mixing index

$$M = \frac{\sigma_0^2 - \sigma^2}{\sigma_0^2 - \sigma_r^2}$$

N-the number of grids being counted c_i-local fraction of sample particles

$\bar{c}$-average fraction of particles in a sample 0-complete separation

r-complete mixing

- **Analyze**

➢ According to the figure above, under the condition of no magnetic, the two-component particles can fully mix at t=3s, and there is no separation trend after that

Two-component particle

☐ Results

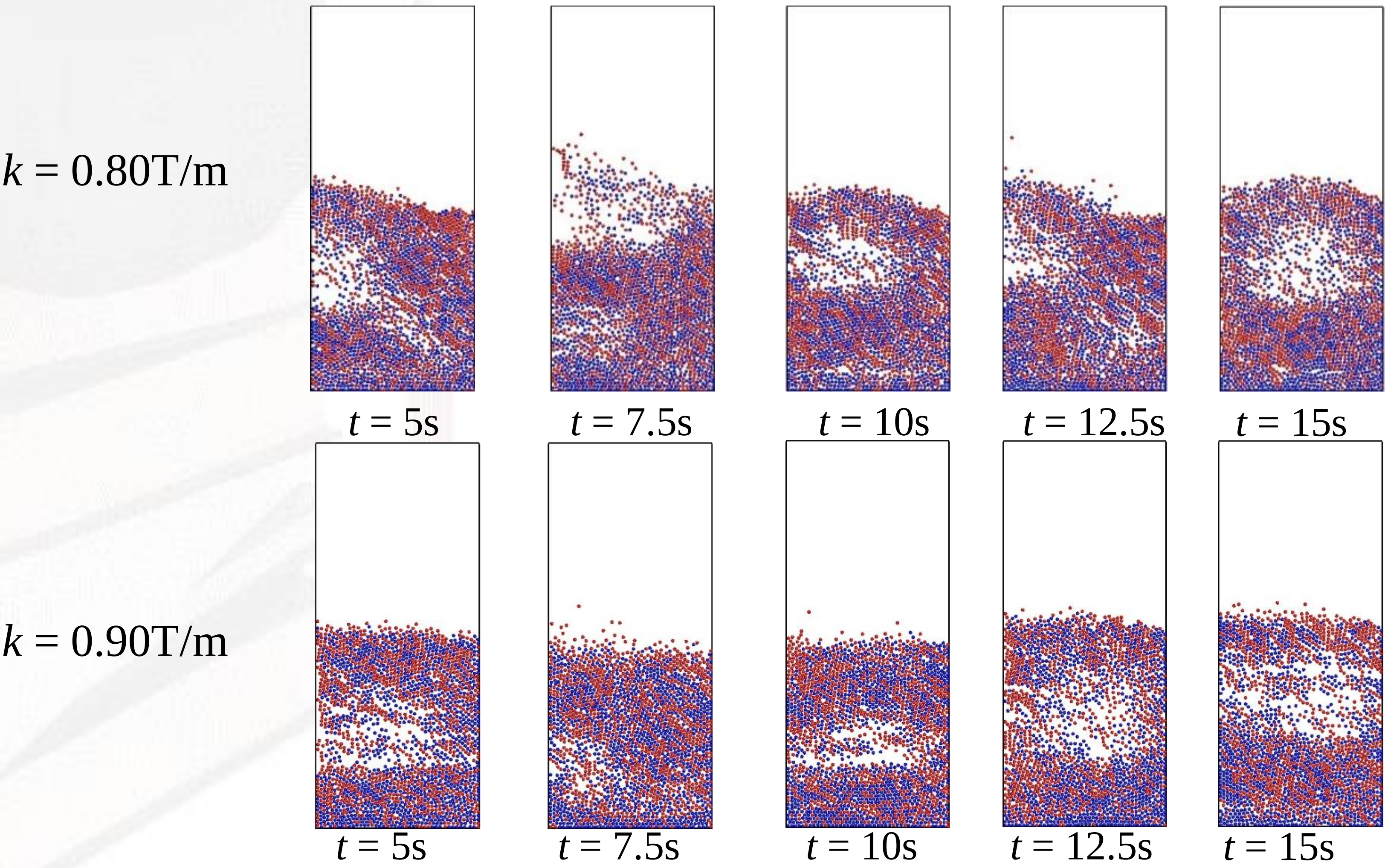

Two-component particle

Results

k =1.00T/m

k =1.10T/m

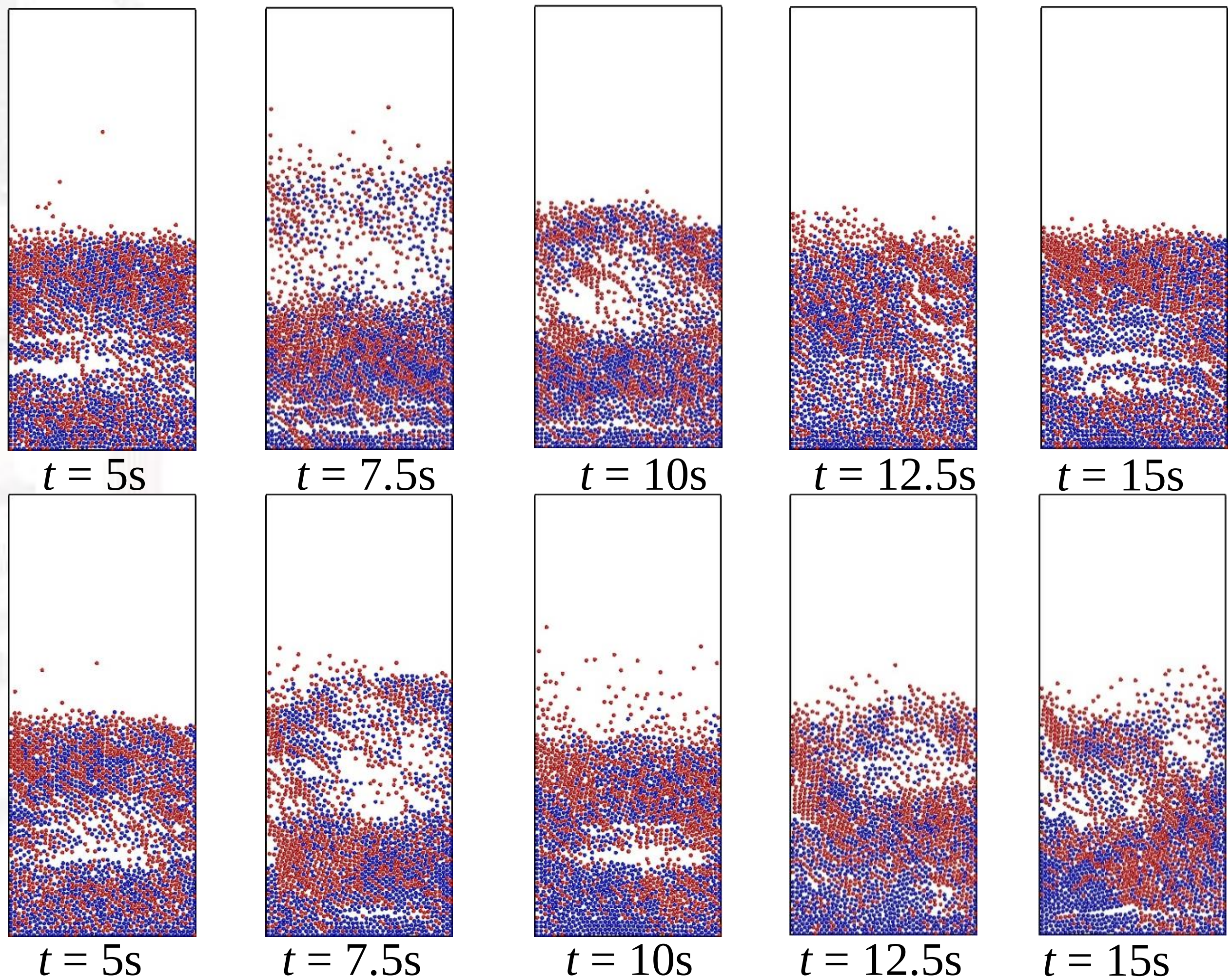

Two-component particle

Results

k=1.20T/m

k=1.30T/m

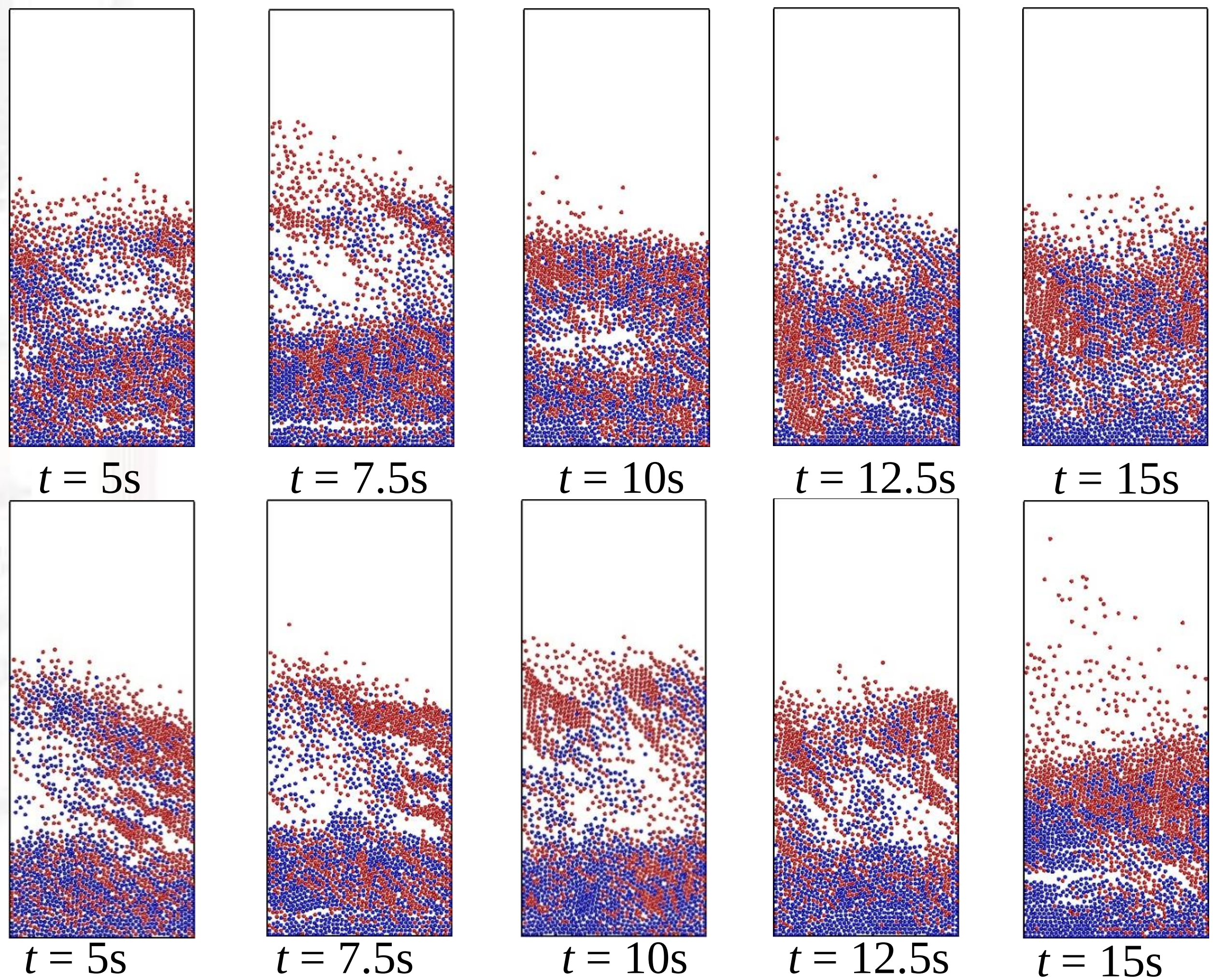

Two-component particle

❑ Results

k =1.40T/m

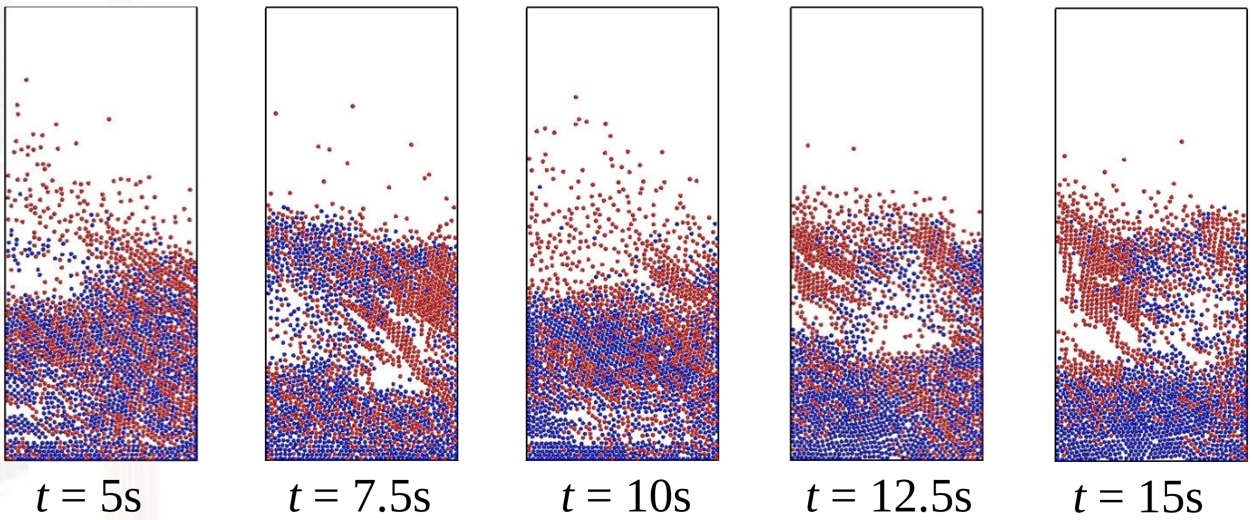

- **Analyze**

➢ According to the instantaneous spatial distribution of 5-15s, the magnetic particles(red) were gradually separated to the upper part of the bed with time

➢ The larger the magnetic field gradient, the more obvious the separation phenomenon

Two-component particle

Results

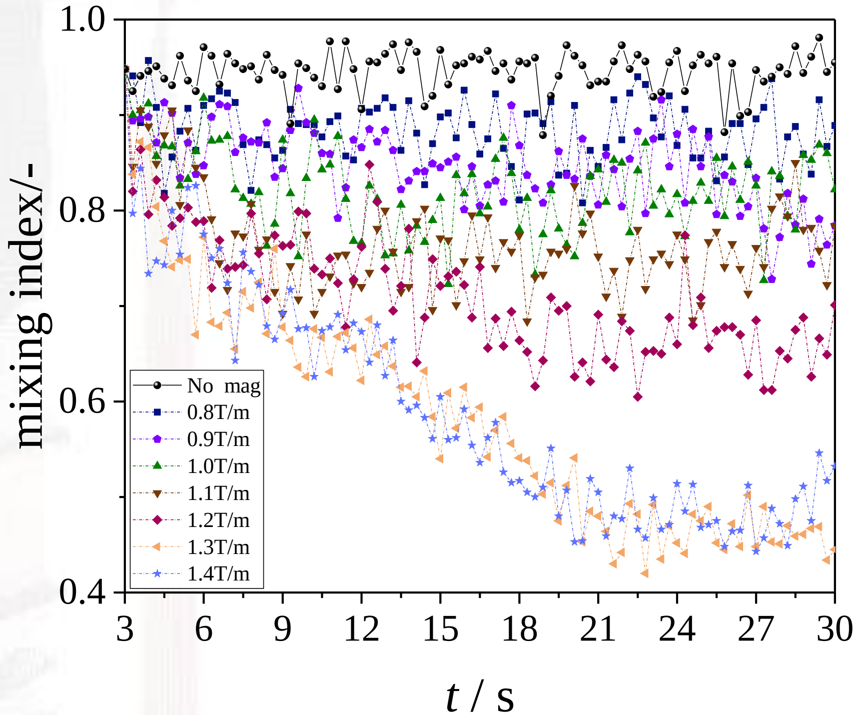

Particle mixing index under different gradient conditions

- **Analyze**

➢ The mixing index of particles in magnetic condition is lower than that in non-magnetic condition

➢ The higher the gradient of gradient magnetic field, the higher the degree of particle separation

CATALOGUE

Conclusion

With taking the ferromagnetic particle system as the research object, the simulation of particle flow characteristics in magnetically controlled gas-solid fluidized bed was carried out.

Single-component particle

- **Uniform magnetic field:** Particles aggregate in chains under the action of a magnetic field, with bubble migration, and obvious ‘gullies’ appear under high magnetic field intensity
- **Gradient magnetic field:** As the magnetic field gradient increases, the bed pressure drop decreases linearly

Two-component particle

- The higher the magnetic field gradient, the higher the separation degree of particles

Thank you for listening